Supporting Information

In-situ Wrapping Si Nanoparticles with 2D Carbon Nanosheets as High-Areal-Capacity Anode for Lithium-Ion Batteries

Lijing Yan[1] *, Jie Liu*[1]*, Qianqian Wang*[1]*, Minghao Sun*[1]*, Zhanguo Jiang*[3]*, Chengdu Liang*[1]*, Feng Pan*[2,*] *and Zhan Lin*[1,3,*]

[1]Zhejiang Provincial Key Laboratory of Advanced Chemical Engineering Manufacture Technology, College of Chemical and Biological Engineering, Zhejiang University, Hangzhou 310027, China

[2]School of Advanced Materials, Peking University, Shenzhen Graduate School, Shenzhen 518055, China

[3]College of Light Industry and Chemical Engineering, Guangdong University of Technology, Guangzhou 510006, China

Email: panfeng@pkusz.edu.cn (F.P.) zhanlin@zju.edu.cn (Z.L.)

Experimental Section.

Material Syntheses. Si/C composites were synthesized via the following route: 0.4 g D-(+)-glucose, 13.5 g KCl, 11.5 g NaCl, 0.164 g NH_4Cl and 0.25 g SiNPs (~50 nm from Alfa-Aesar) for Si/C-0.25 (0.2 g for Si/C-0.2 and 0.3 g for Si/C-0.3, respectively) were mixed uniformly by ball milling at 400 rpm for 20 minutes. Then the powder mixture was filled into ceramic boat and afterwards put into an air circulation oven at 150 °C for 12h, then loaded into a tube furnace equipped with continuous argon flow. After flushing with argon for 30 minutes to eliminate air, the system was ramped at 5 °C min^{-1} to 150 °C and kept at this temperature for 2 h, then continued to heat up to 1050 °C at a rate of 30 °C min^{-1} and kept for 1 h. Finally, the system was cooled to ambient temperature. Meanwhile, the argon flow was maintained until the temperature reached below 30 °C. The block of products were crushed into particles and removed the salts by suction filtration with sufficient amount of ultrapure water for three times. Then as-obtained materials were dried at 60 °C in a vacuum oven for 12 h. For comparison, the pure carbon was synthesized using the same procedure without the addition of SiNPs.

Material Characterizations. The morphology and structure of the samples were investigated by a TEM (Hitachi H-9500) at 300 kV and a field-emission SEM (SU8010 and Zeiss Ultra55) at 5 kV. TGA was performed on a Pyris 1 TGA (Perkin Elmer) System under air flow (100−700 °C, 10 °C min^{-1}). The N_2 adsorption-desorption isotherms were measured by an Autosorb-1-C automatic

surface area analyzer (Quatachrome Corp). XRD patterns were recorded on a Rigaku D/MAX-2550-PC X-ray diffractometer with Cu Kα radiation (λ = 0.154 nm). Raman spectra was collected on a Horiba HR Evolution using a laser with an excitation wavelength of 532 nm.

Electrochemical Tests. The tapped volume of the 0.31g Si/C powders is 2.2 ml, resulting the tap density is 0.141 g cm^{-3}.The electrochemical measurements were carried out using CR2025 coin cells. For half cells, the Si/C working electrode was prepared using the active materials, conductive Super P, and sodium alginate binder in a weight ratio of 70:15:15. The slurry was coated onto a Cu foil and dried in a vacuum oven at 100 °C overnight. The areal mass loading of the active material was 0.75-5.0 mg cm^{-2}. The specific capacities were based on the total weight of the Si/C composite. Lithium chip was used as both counter electrode and reference electrode. The pure carbon half cells were prepared using the same procedure, only replacing the active materials. For fair comparison with the SiNPs, we adjusted the content of Si in Si/C-0.25 to be 53% in the SiNPs electrode. As a result, based on the formula of 70:15:15, the content of additional conducting carbon in the SiNPs electrode is 32%. For full cells, the $Li(Ni_{0.5}Mn_{0.3}Co_{0.2})O_2$ (NMC) cathode was prepared by mixing NMC, Super P, and polyvinylidene difluoride (PVDF) dissolved in *N*-methyl-2-pyrrolidone (NMP) in a ratio of 94:2:4 to form a slurry, which was then pasted on an Al foil and dried under vacuum at 70 °C. The Si/C anode was pre-activated in a half cell after two cycles between 0.01 and 1.2 V at 100 mA g^{-1} to form a stable SEI layer and then taken out as anode for the full cell. Full cell was

obtained by matching the cathode and anode capacity with a ratio of ~1:1.1. The specific capacity was based on the weight of NMC. The electrolyte was composed of 1 M $LiPF_6$ in a mixture of ethylene carbonate, dimethyl carbonate, and diethyl carbonate (1:1:1 in volume) and 10 vol% FEC was added. A Celgard 2400 membrane was used as the separator. All cells were fabricated in an Ar-filled glove box with moisture and oxygen concentrations below 0.1 ppm. Galvanostatic charge–discharge measurements of Si/C half cells were all conducted on a LAND battery tester between 0.01 and 1.2 V, while the full cells were tested between 2.5 and 4.3 V. CV measurements were performed on a Solartron 1480 MultiStat instrument with a scan rate of 0.1 mV s^{-1}. The EIS was measured between 0.01 to 10^5 Hz with an excitation voltage of 5 mV.

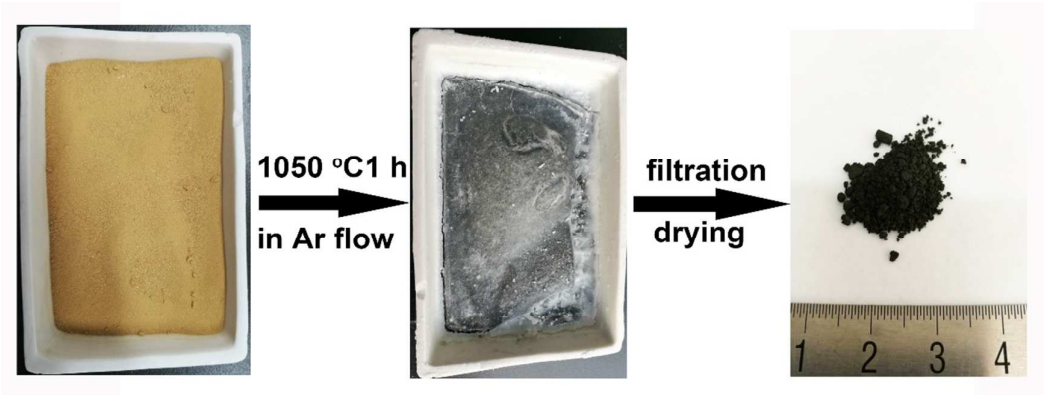

Figure S1. Digital photos of the precursors in ceramic boat before (left) and after (middle) carbonization.

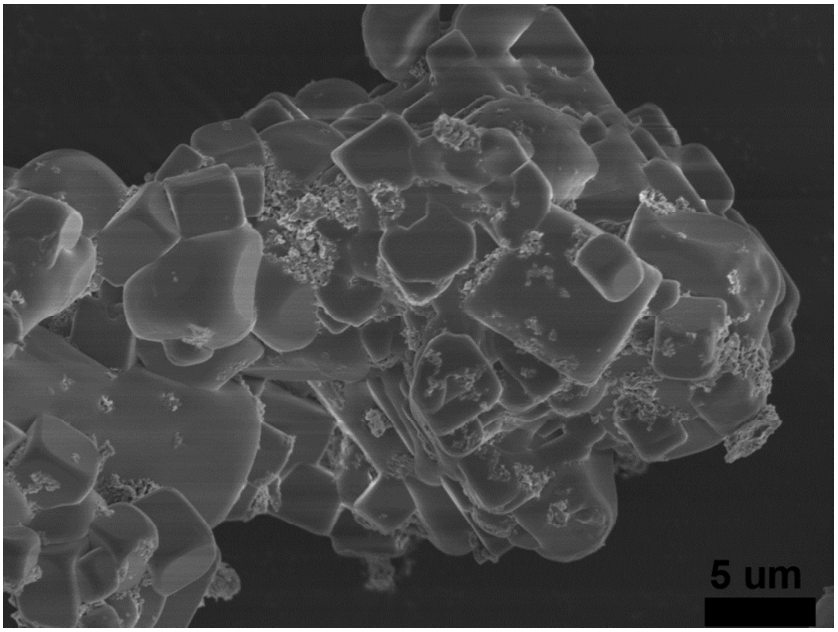

Figure S2. The SEM image of the Si/C composite before removing NaCl and KCl.

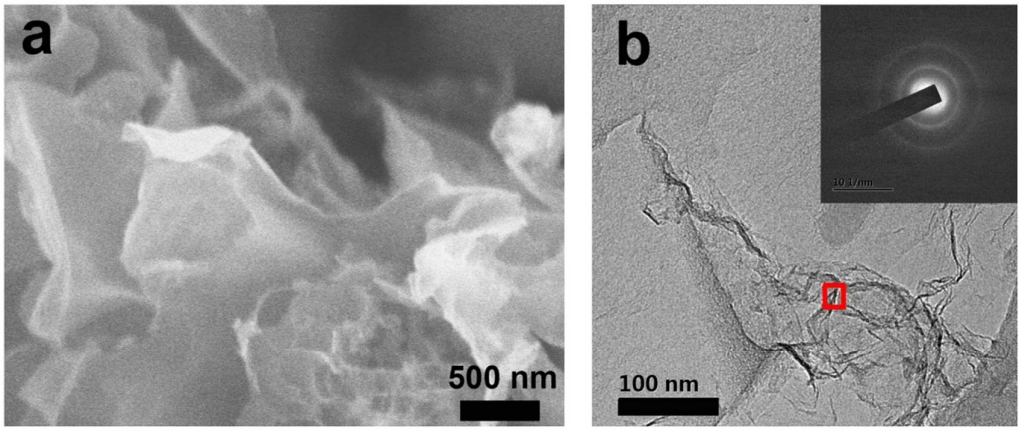

Figure S3. (a) SEM image and (b) TEM image of the pure carbon. The inset: the SAED pattern taken from the red box.

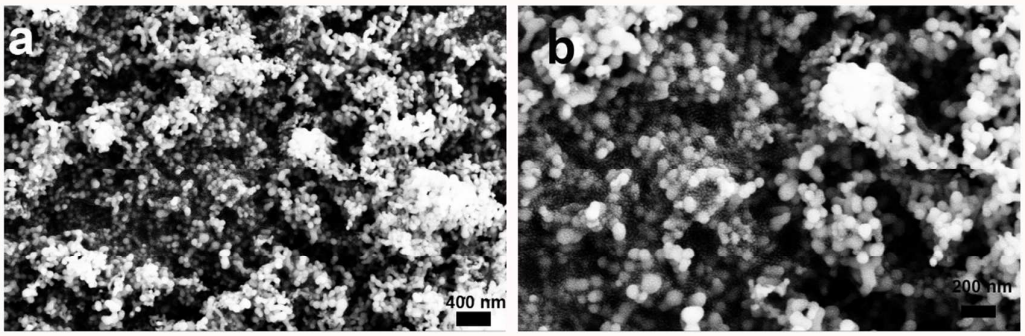

Figure S4. (a) and (b) SEM images of the commercial SiNPs at different magnifications.

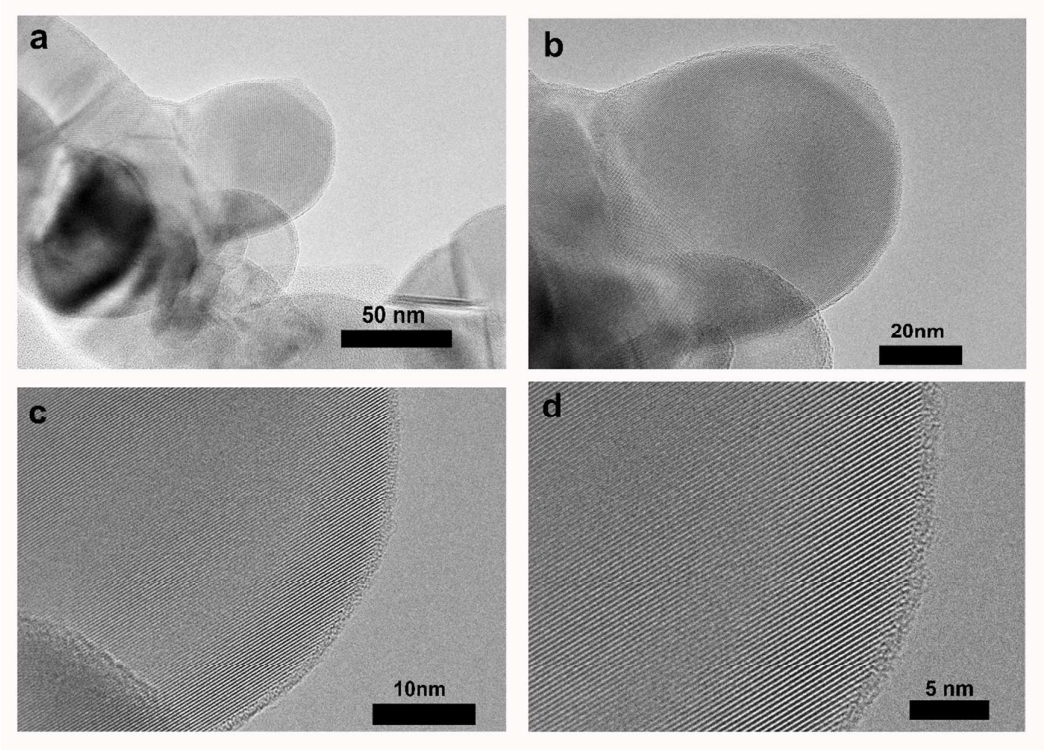

Figure S5. (a) and (b) TEM images, (c) and (d) HRTEM images of the SiNPs at different magnifications.

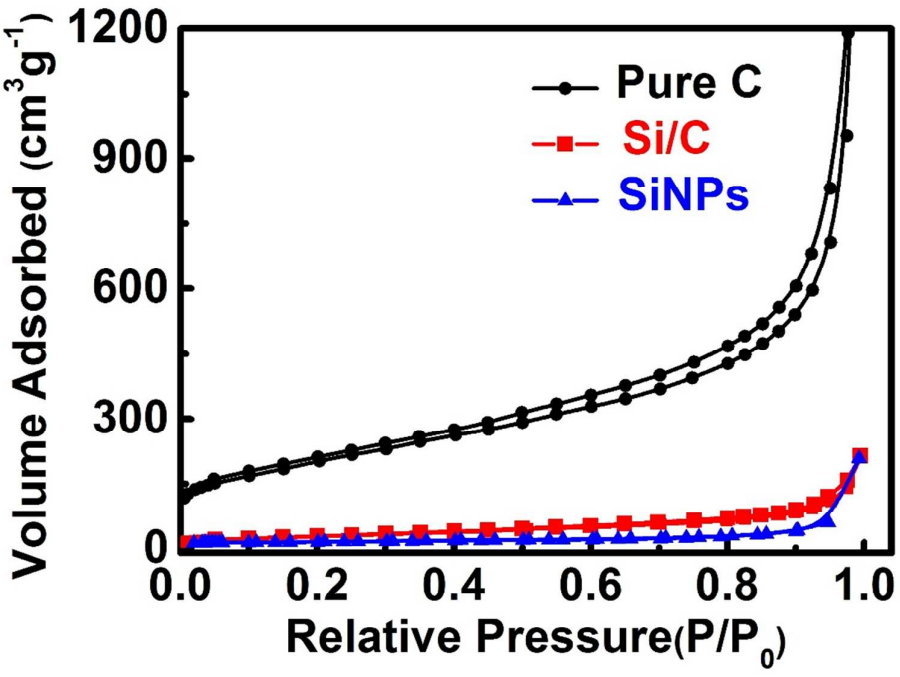

Figure S6. N_2 adsorption-desorption isotherms of the as-fabricated Si/C composite ,SiNPs and Pure C.

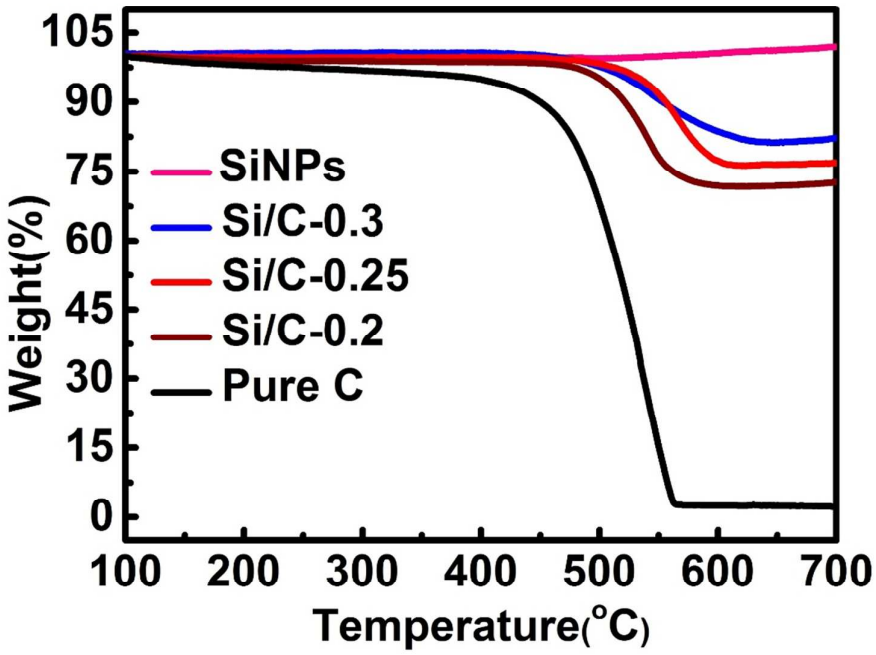

Figure S7. TGA curves of the SiNPs, Si/C composites in certain ratio and Pure C in air between 100 and 700 ^{o}C with a heating rate of 10 ^{o}C min^{-1}.

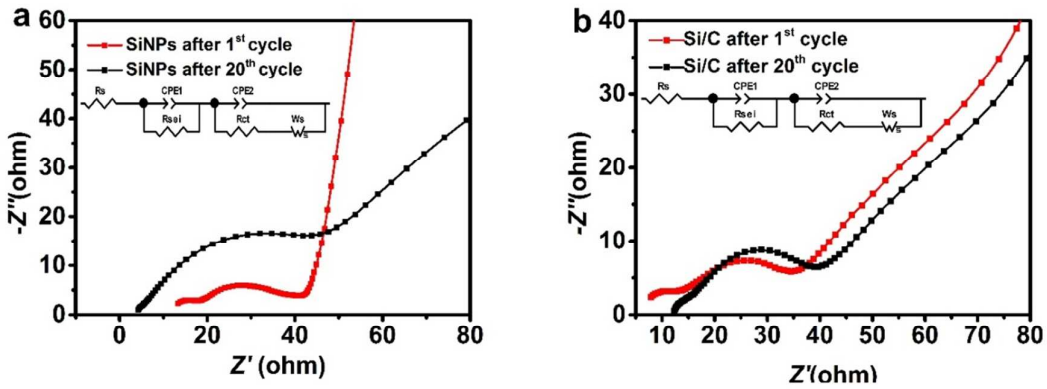

Figure S8. (a) Nyquist plots of the SiNPs electrode after 1st and 20th cycle. (b) Nyquist plots of the Si/C electrode after 1st and 20th cycle. (a) and (b) are both obtained from EIS within 100 kHz to 0.01 Hz (perturbation voltage: 5 mV).

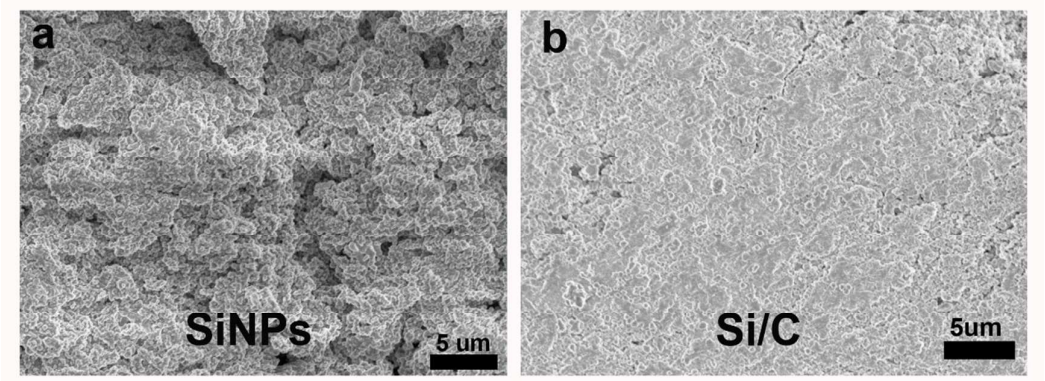

Figure S9. SEM images of (a) the SiNPs electrode surface after the 1st cycle and (b) the Si/C electrode surface after 1st cycle.

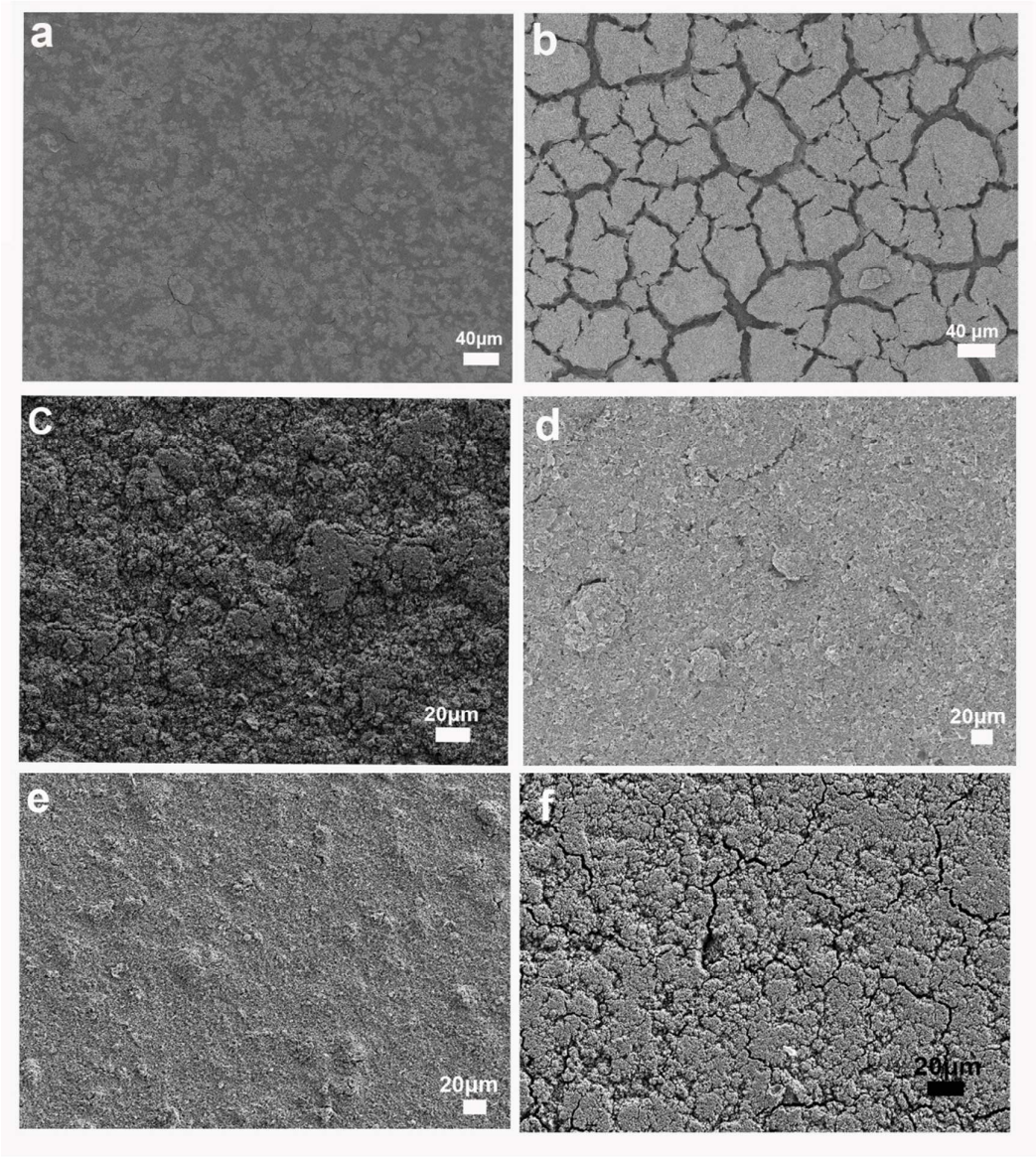

Figure S10. SEM image of the SiNPs electrode (a) before cycling and (b) after the 1st cycle. The Si/C composite electrode (c) before cycling, (d) after the 1st cycle, (e) after 120 cycles and (f) after 500 cycles at a current density of 420 mA g^{-1}.

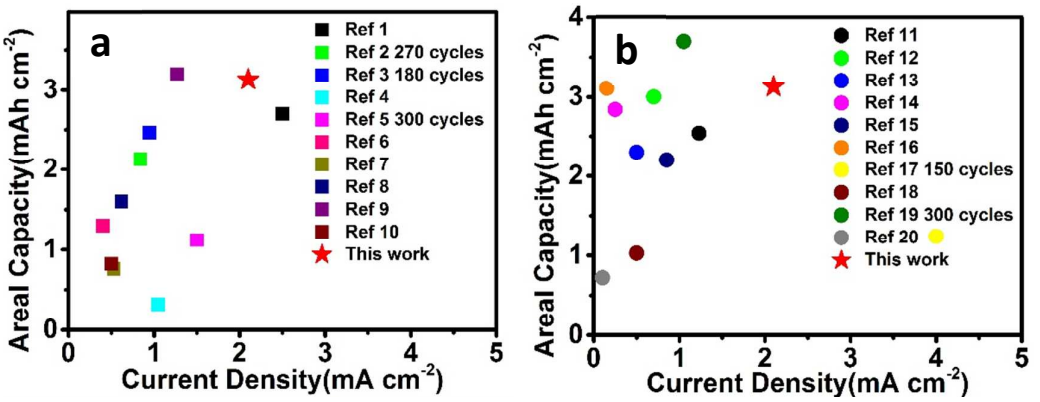

Figure S11. Comparsion of the as-prepared Si/C composites with the (a) Si/Graphene composites, (b) Si/C composites. The references are all representative outstanding research results in the past three years about Si/Graphene or Si/C composites as anode for LIBs.

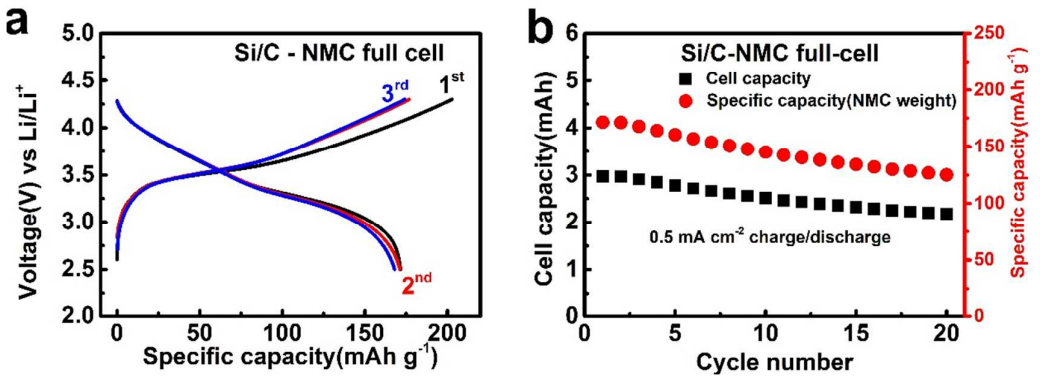

Figure S12. Electrochemical performance of a typical $Li(Ni_{0.5}Mn_{0.3}Co_{0.2})O_2$ –Si/C full cell. (a) Charge-discharge curves. (b) Cycling performance of the full cell.

Table S1. Impedance parameters for SiNPs and Si/C electrodes before cycling, after the 1st and 20th cycles.

Electrode	Rs/Ω	Rsei/Ω	Rct/Ω
SiNPs before cylcing	3.33	none	233.50
Si/C before cycling	3.53	none	183.10
SiNPs after the 1st cycle	11.07	6.85	21.86
SiNPs after the 20th cycle	3.75	52.55	137.90
Si/C after the 1st cycle	5.74	4.05	37.41
Si/C after the 20th cycle	9.04	57.21	9.80

Table S2. Comparisons of Si/2D carbon nanosheet composite anode to different Si/graphene composite electrodes. The mass loading are all based on the weight of silicon and graphene.

Current density (mA cm^{-2})	Potential range (V)	Mass loading (mg cm^{-2})	Cycle number	Areal capacity (mAh cm^{-2})	Reference
2.10	0.01-1.2	5.00	100	3.13	This work
2.50	0.01-1.5	2.50	100	2.70	[1]
0.84	0.005-2.0	2.10	270	2.13	[2]
0.95	0.01-1.0	1.90	180	2.46	[3]
1.05	0.01-1.5	0.35	100	0.32	[4]
1.50	0.01-1	0.80	300	1.12	[5]
0.40	0.01-1.5	1.80	200	1.30	[6]
0.53	0.01-1.5	0.53	100	0.76	[7]
0.62	0.05-1.5	1.10	100	1.60	[8]
1.27	0.01-1.0	3.18	100	3.20	[9]
0.50	0.01-1.0	1.00	100	0.82	[10]

Table S3. Comparisons of Si/2D carbon nanosheet composite anode to different Si/C electrodes with high mass loadings and high areal capacities. The mass loading are all based on the weight of silicon and carbon.

Current density (mA cm^{-2})	Potential range (V)	Mass loading (mg cm^{-2})	Cycle number	Areal capacity (mAh cm^{-2})	Reference
2.10	0.01-1.2	5.00	100	3.13	This work
1.23	0.005-1.0	4.10	100	2.54	[11]
0.70	0.01-1.0	3.12	100	3.00	[12]
0.50	0.01-1.0	2.02	100	2.30	[13]
0.25	0.01-1.0	2.01	100	2.84	[14]
0.85	0.02-1.5	1.70	100	2.20	[15]
0.15	0.01-2.0	3.00	100	3.11	[16]
4.00	0.01-1.2	1.00	150	1.24	[17]
0.50	0.01-1.5	1.00	100	1.03	[18]
1.05	0.02-1.2	2.10	300	3.70	[19]
0.10	0.01-1.0	1.00	100	0.72	[20]

References:

(1) Son, I. H.; Hwan Park, J.; Kwon, S.; Park, S.; Rummeli, M. H.; Bachmatiuk, A.; Song, H. J.; Ku, J.; Choi, J. W.; Choi, J. M.; Doo, S. G.; Chang, H. Silicon Carbide-Free Graphene Growth on Silicon for Lithium-Ion Battery with High Volumetric Energy Density. *Nat. Commun.* **2015,** *6*, 7393.

(2) Jing, S.; Jiang, H.; Hu, Y.; Shen, J.; Li, C. Face-to-Face Contact and Open-Void Coinvolved Si/C Nanohybrids Lithium-Ion Battery Anodes with Extremely Long Cycle Life. *Adv. Funct. Mater.* **2015,** *25*, 5395-5401.

(3) Ma, Y.; Younesi, R.; Pan, R.; Liu, C.; Zhu, J.; Wei, B.; Edström, K. Constraining Si Particles within Graphene Foam Monolith: Interfacial Modification for High-Performance Li^+ Storage and Flexible Integrated Configuration. *Adv. Funct. Mater.* **2016,** *26*, 6797-6806.

(4) Suresh, S.; Wu, Z. P.; Bartolucci, S. F.; Basu, S.; Mukherjee, R.; Gupta, T.; Hundekar, P.; Shi, Y.; Lu, T.-M.; Koratkar, N. Protecting Silicon Film Anodes in Lithium-Ion Batteries Using an Atomically Thin Graphene Drape. *Acs Nano* **2017,** *11*, 5051-5061.

(5) Li, Y.; Yan, K.; Lee, H. W.; Lu, Z.; Liu, N.; Cui, Y. Growth of Conformal Graphene Cages on Micrometre-Sized Silicon Particles as Stable Battery Anodes. *Nat. Energy* **2016,** *1*, 15029.

(6) Hu, R.; Sun, W.; Chen, Y.; Zeng, M.; Zhu, M. Silicon/Graphene Based Nanocomposite Anode: Large-Scale Production and Stable High Capacity for Lithium Ion Batteries. *J. Mater. Chem. A* **2014,** *2*, 9118-9125.

(7) Liu, X.; Zhang, J.; Si, W.; Xi, L.; Eichler, B.; Yan, C.; Schmidt, O. G. Sandwich Nanoarchitecture of Si/Reduced Graphene Oxide Bilayer Nanomembranes for Li-Ion Batteries with Long Cycle Life. *Acs Nano* **2015,** *9*, 1198-1205.

(8) Feng, K.; Ahn, W.; Lui, G.; Park, H. W.; Kashkooli, A. G.; Jiang, G.; Wang, X.; Xiao, X.; Chen, Z. Implementing an in-Situ Carbon Network in Si/Reduced Graphene Oxide for High Performance Lithium-Ion Battery Anodes. *Nano Energy* **2016,** *19*, 187-197.

(9) Yi, R.; Zai, J.; Dai, F.; Gordin, M. L.; Wang, D. Dual Conductive Network-Enabled Graphene/Si–C Composite Anode with High Areal Capacity for Lithium-Ion Batteries. *Nano Energy* **2014,** *6*, 211-218.

(10) Maroni, F.; Raccichini, R.; Birrozzi, A.; Carbonari, G.; Tossici, R.; Croce, F.; Marassi, R.; Nobili, F. Graphene/Silicon Nanocomposite Anode with Enhanced Electrochemical Stability for Lithium-Ion Battery Applications. *J. Power Sources* **2014,** *269*, 873-882.

(11) Xu, Q.; Li, J.-Y.; Sun, J.-K.; Yin, Y.-X.; Wan, L.-J.; Guo, Y.-G. Watermelon-Inspired Si/C Microspheres with Hierarchical Buffer Structures for Densely Compacted Lithium-Ion Battery Anodes. *Adv. Energy. Mater.* **2017,** *7*, 1601481.

(12) Liu, N.; Lu, Z.; Zhao, J.; McDowell, M. T.; Lee, H. W.; Zhao, W.; Cui, Y. A Pomegranate-Inspired Nanoscale Design for Large-Volume-Change Lithium Battery Anodes. *Nat. Nanotech.* **2014,** *9*, 187-192.

(13) Lin, D.; Lu, Z.; Hsu, P.-C.; Lee, H. R.; Liu, N.; Zhao, J.; Wang, H.; Liu, C.; Cui, Y. A High Tap Density Secondary Silicon Particle Anode Fabricated by Scalable Mechanical Pressing for Lithium-Ion Batteries. *Energy Environ. Sci.* **2015,** *8*, 2371-2376.
(14) Lu, Z.; Liu, N.; Lee, H. W.; Zhao, J.; Li, W.; Li, Y.; Cui, Y. Nonfilling Carbon Coating of Porous Silicon Micrometer-Sized Particles for High-Performance Lithium Battery Anodes. *Acs Nano* **2015,** *9*, 2540-2547.
(15) Xu, Y.; Zhu, Y.; Han, F.; Luo, C.; Wang, C. 3d Si/C Fiber Paper Electrodes Fabricated Using a Combined Electrospray/Electrospinning Technique for Li‐Ion Batteries. *Adv. Energy. Mater.* **2015,** *5,* 1400753.
(16) Zhang, Z.; Wang, Y.; Ren, W.; Tan, Q.; Chen, Y.; Li, H.; Zhong, Z.; Su, F. Scalable Synthesis of Interconnected Porous Silicon/Carbon Composites by the Rochow Reaction as High-Performance Anodes of Lithium Ion Batteries. *Angew. Chem. Int. Ed.* **2014,** *53*, 5165-5169.
(17) Jung, D. S.; Hwang, T. H.; Park, S. B.; Choi, J. W. Spray Drying Method for Large-Scale and High-Performance Silicon Negative Electrodes in Li-Ion Batteries. *Nano Lett.* **2013,** *13*, 2092-2097.
(18) Zhang, Y. C.; You, Y.; Xin, S.; Yin, Y. X.; Zhang, J.; Wang, P.; Zheng, X. S.; Cao, F. F.; Guo, Y. G. Rice Husk-Derived Hierarchical Silicon/Nitrogen-Doped Carbon/Carbon Nanotube Spheres as Low-Cost and High-Capacity Anodes for Lithium-Ion Batteries. *Nano Energy* **2016,** *25*, 120-127.
(19) Zhang, R.; Du, Y.; Li, D.; Shen, D.; Yang, J.; Guo, Z.; Liu, H. K.; Elzatahry, A. A.; Zhao, D. Highly Reversible and Large Lithium Storage in Mesoporous Si/C Nanocomposite Anodes with Silicon Nanoparticles Embedded in a Carbon Framework. *Adv. Mater.* **2014,** *26*, 6749-6755.
(20) Sun, Y.; Lopez, J.; Lee, H. W.; Liu, N.; Zheng, G.; Wu, C. L.; Sun, J.; Liu, W.; Chung, J. W.; Bao, Z. A Stretchable Graphitic Carbon/Si Anode Enabled by Conformal Coating of a Self-Healing Elastic Polymer. *Adv. Mater.* **2016,** *28*, 2455-2461.